EPITHELIAL WATER TRANSPORT IN A BALANCED GRADIENT SYSTEM

RICHARD T. MATHIAS
Department of Physiology, Rush Medical College, Chicago, Illinois 60612

ABSTRACT The relationship between epithelial fluid transport, standing osmotic gradients, and standing hydrostatic pressure gradients has been investigated using a perturbation expansion of the governing equations. The assumptions used in the expansion are: (*a*) the volume of lateral intercellular space per unit volume of epithelium is small; (*b*) the membrane osmotic permeability is much larger than the solute permeability. We find that the rate of fluid reabsorption is set by the rate of active solute transport across lateral membranes. The fluid that crosses the lateral membranes and enters the intercellular cleft is driven longitudinally by small gradients in hydrostatic pressure. The small hydrostatic pressure in the intercellular space is capable of causing significant transmembrane fluid movement, however, the transmembrane effect is countered by the presence of a small standing osmotic gradient. Longitudinal hydrostatic and osmotic gradients balance such that their combined effect on transmembrane fluid flow is zero, whereas longitudinal flow is driven by the hydrostatic gradient. Because of this balance, standing gradients within intercellular clefts are effectively uncoupled from the rate of fluid reabsorption, which is driven by small, localized osmotic gradients within the cells. Water enters the cells across apical membranes and leaves across the lateral intercellular membranes. Fluid that enters the intercellular clefts can, in principle, exit either the basal end or be secreted from the apical end through tight junctions. Fluid flow through tight junctions is shown to depend on a dimensionless parameter, which scales the resistance to solute flow of the entire cleft relative to that of the junction. Estimates of the value of this parameter suggest that an electrically leaky epithelium may be effectively a tight epithelium in regard to fluid flow.

INTRODUCTION

One of the numerous functions of epithelia is to transport water. It is generally believed that water molecules per se are not actively transported; rather, water movement is a passive consequence of the active transport of solutes. The movement of water, therefore, requires a macroscopic driving force such as an osmotic or hydrostatic gradient, yet some of the most vigorous flows of water occur with no measurable transepithelial gradients. Moreover, the fluid transported by these epithelia appears to be essentially isotonic; hence water is passively moving in the absence of any measured driving force.

Curran (1960) proposed that a three-compartment model would account for the above observations, and Kaye et al. (1966) suggested the lateral intercellular spaces as the intermediate compartment in Curran's model. These ideas were analyzed by Diamond and Bossert (1967), who proposed that standing osmotic gradients in the lateral intercellular spaces provide the driving force for fluid transport. However, the standing osmotic gradient model has been the subject of some criticism, e.g., Hill (1975). Moreover, when modern parameter values have been used in recent models (reviewed in the Discussion), large-standing osmotic gradients have not been predicted.

Balanced Gradient Model

This paper extends the analysis of Diamond and Bossert (1967) of the role of small lateral intercellular spaces in the transport of water. However, the conclusions of this analysis are somewhat different, presumably because several additional factors are considered: (*a*) the location of active transport is assumed to be uniform along the membranes of the intercellular clefts (Sterling, 1972 or Kyte, 1976); (*b*) the leakiness or tightness of the apical intercellular junctions is allowed to be a variable parameter (see the discussion by Schultz, 1977): (*c*) hydrostatic pressure gradients, across membranes and down intercellular clefts, are explicitly analyzed.

Several other factors are omitted from this analysis. The effects of voltage gradients (Sackin and Boulpaep, 1975; Weinstein and Stephenson, 1979; Weinstein, 1983; McLaughlin and Mathias, 1985) are not considered here. Moreover, the effects of the basement membrane on fluxes are neglected (this assumption is criticized by Sackin and Boulpaep, 1975). Lastly, we assume the conditions on either side of the epithelium are symmetrical. When conditions are asymmetrical, there will be accumulation/depletion of solute in the vicinity of the tight junction, and this situation is not analyzed.

BIOPHYS. J. © Biophysical Society · 0006-3495/85/06/823/14 $1.00
Volume 47 June 1985 823-836

The analysis is done in three stages. Appendix A derives differential equations for fluid flow and solute flux along small lateral intercellular spaces. This stage exploits the smallness of the ratio of cleft width/cleft length to simplify the fluid dynamic equations. The resulting approximate transport laws are similar to those presented in Huss and Marsh (1975), but in this analysis the morphometric parameters that characterize an epithelium (e.g., Welling and Welling, 1975) are explicitly included. Appendix B extends the analysis in Appendix A to include the cells as well as the intercellular spaces and uses a perturbation expansion to solve the transport equations. This expansion differs from that used by Segel (1970) in that: hydrostatic pressure is included in the equations, flux through cells is considered, and the expansion depends on the smallness of the lateral spaces relative to cell size and on the largeness of the membrane osmotic permeability relative to solute permeability (see Eq. 11). In the text, the results of Appendix B are used to derive simple differential equations for the situation where intercellular clefts are more dilated. These equations are similar to those presented in Weinstein and Stephenson (1981) but differ inasmuch as hydrostatic pressure and explicit dependence of the fluxes on the morphometry of the tissue are included. The results of the perturbation expansion are applied to the epithelium of mammalian proximal tubule and the predicted osmotic and hydrostatic gradients are examined.

Emergent Osmolarity

The osmolarity of the bulk solution moving within a lateral intercellular cleft is calculated by dividing the solute flux $j_e(x)$ by the water flux $u_e(x)$ (Diamond and Bossert, 1967). The solute flux is due to diffusion of solute down its concentration gradient, dc_e/dx, plus convection of solute by water flowing down a hydrostatic pressure gradient, dp_e/dx, whereas water flux depends only upon the hydrostatic gradient

$$\mathrm{os}(x) = \frac{D_e \frac{dc_e(x)}{dx} + c_e(x) \frac{1}{\rho_e} \frac{dp_e(x)}{dx}}{\frac{1}{\rho_e} \frac{dp_e(x)}{dx}}, \tag{1}$$

where D_e is the effective diffusion coefficient for solute within the cleft and ρ_e is the effective resistance of clefts to water flow (see Appendix A).

The importance of each component of Eq. 1 is more easily assessed if the parameters are normalized. The following normalization provides the desired nondimensional equation

$$\begin{aligned} C_e &= c_e/c_o; \\ \mathrm{Os} &= \mathrm{os}/c_o; \\ P_e &= p_e/RTc_o; \\ X &= x/\ell; \end{aligned} \tag{2}$$

where c_o is the concentration or osmolarity of solute in the bulk solution on either side of the epithelium and ℓ is the thickness of the epithelium. Substituting Eq. 2 into Eq. 1 gives

$$\mathrm{Os}(X) = \frac{\delta_e \frac{dC_e(X)}{dX} + C_e(X) \frac{dP_e(X)}{dX}}{\frac{dP_e(X)}{dX}}, \tag{3}$$

where δ_e scales the relative contribution of diffusion vs. convection:

$$\delta_e = \frac{\rho_e D_e}{RTc_o}. \tag{4}$$

If δ_e is small, then the flow tends to be dominated by convection. Table I shows δ_e is indeed a small number for mammalian proximal tubule ($\delta_e \approx 10^{-2}$). Hence, as $C_e(X)$ is near unity, if we have a balanced gradient situation where

$$\frac{dC_e(X)}{dX} \approx \frac{dP_e(X)}{dX}, \tag{5}$$

then convection will always dominate. And when convection dominates, it is easy to see that the emergent osmolarity will always approach isotonic.

The emergent solution is isotonic by definition when $\mathrm{Os}(1) = 1$. One of the boundary conditions on the problem is that $c_e(x = \ell) = c_o$ or equivalently $C_e(1) = 1$, so if we evaluate Eq. 3 at $X = 1$, we find that there are two conditions whereupon $\mathrm{Os}(1) \rightarrow 1$: either

$$\delta_e \rightarrow 0 \tag{6}$$

or

$$\frac{dC_e(1)}{dX} \rightarrow 0. \tag{7}$$

In the standing osmotic gradient model of Diamond and Bossert (1967), the second condition (Eq. 7) was achieved by placing the site of active transport, and therefore the standing osmotic gradient, near to $X = 0$ and far from $X = 1$. The analysis presented here suggests that hydrostatic and osmotic gradients will balance everywhere along the cleft, hence transport approaches isotonic by virtue of the smallness of δ_e (Eq. 6), and is therefore independent of the site of solute transport.

The parameters appearing in the dimensional equations here and elsewhere are generically classified as given in the Glossary. The parameters in the Glossary can be identified with the appropriate location within the epithelium by the subscript given in the section Subscripts. Many of the parameters are illustrated in Fig. 1.

GLOSSARY

c concentration or osmolarity of solute (mol/cm^3);
D effective diffusion coefficient for solute (cm^2/s);

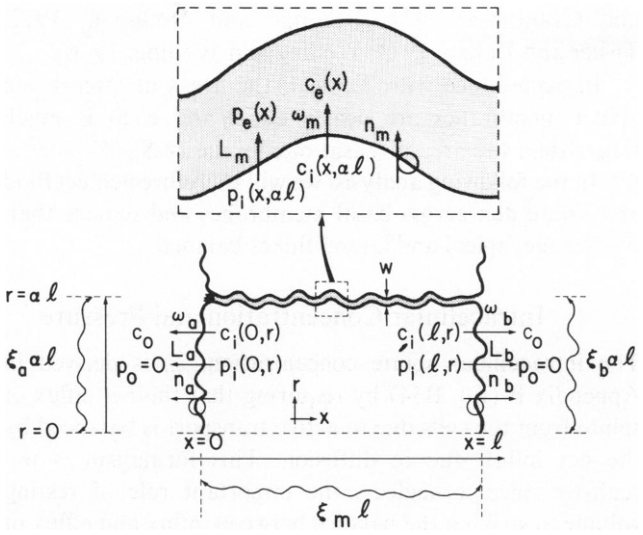

FIGURE 1 The most important pathways whereby water and solute cross membranes. The cells are assumed to be right circular cylinders in shape but to have a wavy surface, which increases the area for transmembrane flux. The length of the cylinder is ℓ and the radius $\alpha\ell$. The clefts between cells have width w and extend across the epithelium. At the basal side (subscripted b) the clefts are assumed to be open to the bath, whereas a tight junction is assumed to occlude the apical end. In the analysis, the actual permeability of the junction is allowed to be a variable parameter.

- j flux density of solute (mol/[cm^2 s]);
- L hydraulic conductivity of a membrane (cm/[s mmHg]);
- n active transmembrane solute transport (mol/[cm^2 s]);
- p hydrostatic pressure (mmHg)
- u flow velocity of water (cm/s);
- ξ wiggle factor giving the length of membrane per unit length of idealized geometry;
- π net transmembrane osmotic pressure (mM);
- ρ effective resistance to water flow (mmHg/[cm^2 s]);
- σ membrane reflection coefficient; and
- ω membrane permeability to solute (cm/s).

Subscripts

- a, b apical, basal membranes;
- i, e intracellular space, extracellular space between cells;
- o outside of the tissue in the solution bathing the apical and basal faces;
- t tight junctions between cells;
- m membranes lining the extracellular clefts.

Morphological Parameters

- ℓ the average thickness of the epithelium (cm);
- S_m/V_T the average surface area of lateral membrane in a unit volume of tissue (cm^{-1});
- V_C/V_T the average volume of lateral intercellular clefts in a unit volume of tissue;
- $\alpha\ell$ the average radius of a cell (cm).

THEORY

Equations of Flux

The equations for solute and water flow along the lateral intercellular clefts are derived in Appendix A and are essentially one-dimensional transmission-line-like relationships between flows and forces. These simplified equations could be derived because the width of a cleft is much smaller than its length, and in such a geometry several very good approximations are possible. The dimensions of the cells are relatively equal however (see Fig. 1), so no a priori simplifications of the intracellular problem are possible. Analysis of the intracellular water flow problem in Appendix B begins with the Navier-Stokes equation for conservation of energy and momentum in an incompressible viscous fluid (see Eq. B5), and the water and solute flows must obey equations for conservation of matter.

The complete equations and approximate analytical solutions are derived in Appendix B for the situation where the lateral intercellular spaces are narrow, perhaps <0.02 μm in width. In this situation, the resistance of the clefts to longitudinal water flow is large. Hence, if we define the length constant for fluid flow in accordance with Eq. 12,

$$\lambda_w = 1/\left(\rho_e \frac{S_m}{V_T} L_m\right)^{1/2}, \tag{8}$$

then the value of λ_w^2/ℓ^2 is small.

In epithelia that are vigorously transporting fluid, the intercellular spaces are often dilated (Kaye et al., 1966), hence the resistance to longitudinal fluid flow is less and the value of λ_w^2/ℓ^2 may not be small. Thus the equations for our first-order approximation to intercellular flow will be modified in this situation. In Appendix B we found that standing intercellular osmotic gradients are generally small. We can therefore write

$$c_e(x) = c_o + \delta c_e(x).$$

In clefts wider than 0.02 μm it is reasonable to follow the approximation made by Segel (1970) and Weinstein and Stephenson (1981) that the flux of solute due to convection is approximately

$$u_e(x)c_e(x) \simeq u_e(x)c_o. \tag{9}$$

Furthermore, the wider the cleft the smaller the value of δ_e and the more convection dominates diffusion. We can therefore neglect the solute flux due to diffusion and assume

$$\delta_e \approx 0. \tag{10}$$

Lastly, we will follow the perturbation expansion and assume the membrane osmotic permeability is much larger than the solute permeability:

$$\sigma_m \simeq 1.0, \qquad \omega_m/(RTc_oL_m) \ll 1.0. \tag{11}$$

With the assumptions in Eqs. 9–11, Eqs. B3 and B4 simplify to

$$\frac{d^2p_e(x)}{dx^2} = -\frac{1}{\lambda_w^2}\{p_i - p_e(x) + RT[c_e(x) - c_i]\},$$

$$\frac{1}{\rho_e}\frac{d}{dx}\left(c_o\frac{dp_e}{dx}\right) = -\frac{S_m}{V_T}n_m, \tag{12}$$

and the appropriate boundary conditions are

$$p_e(\ell) = 0, \qquad c_e(\ell) = c_o,$$

$$\frac{c_o}{\rho_e}\frac{dp_e(0)}{dx} = \xi_i^2\omega_i[c_e(0) - c_o]. \tag{13}$$

The above equations are linear and can be solved to obtain

$$p_e(x) = RT[c_e(x) - c_o]$$

$$c_e(x) = c_o + \frac{1}{2}c_o\frac{2}{\alpha}N_m\left\{1 - x^2/\ell^2 - \frac{\Omega_t}{1+\Omega_t}(1 - x/\ell)\right\}, \quad (14)$$

where

$$\frac{2}{\alpha}N_m = \frac{\ell^2\rho_e}{RTc_o^2}\frac{S_m}{V_T}n_m$$

$$\Omega_t = \frac{\ell\rho_e}{RTc_o}\xi_i^2\omega_t. \quad (15)$$

If we compare the above analysis to the solution in Appendix B, we find that Eq. B36 reduces to Eq. 14 in the limits where $\delta_e << 1.0$ and $(2/\alpha)N_m << 1.0$. A small value of δ_e clearly implies convection dominates diffusion. The physical consequences of the normalized rate of solute transport being small are that the rate of fluid transport is small, the intercellular hydrostatic pressure is therefore small, and the balanced gradient in intercellular concentration is also small. The linear convection approximation in Eq. 9 thus depends on the smallness of $(2/\alpha)N_m$. The solution derived in Appendix B appears to be more general than Eq. 14, since in the Appendix diffusion may or may not be important and deviations from the linear convection assumption are allowed.

RESULTS

When considering the behavior and implications of the various results, it is useful to have estimates of the sizes of terms that appear in the equations. The surface areas of membrane and cell dimensions reported in Table I are from Welling and Welling (1975 and 1976) for rabbit proximal tubule. The value of L_m is taken from the review by Spring (1983) where he reports the specific water permeability, P_{osm}, of membranes from *Necturus* gallbladder, where $RTL_m = P_{osm}/V_w$ and $V_w = 55$ mol/l is the partial molar volume of water. His values fall into the range $10^{-9} < L_m < 10^{-8}$ (cm/s)/mmHg and we have chosen the larger limit for mammalian proximal tubule. The value of w in Table I is representative of several preparations, including mammalian proximal tubule (Burg and Grantham, 1971; Berridge and Oschman, 1972; Tisher and Kokko, 1974; Welling and Welling, 1976).

In accordance with Table I, the areas of lateral and apical membranes are nearly equal and each is much larger than the area of basal membrane ($\ell S_m/V_T \approx \xi_a^2 \gg \xi_b^2$). In the following analysis, we will therefore neglect fluid and solute flux across basal membranes and require that, on average, apical and lateral fluxes balance.

Intracellular Concentration and Pressure

The intracellular solute concentration, c_i, is derived in Appendix B (Eq. B34) by requiring that the net efflux of solute from the cells due to active transport is balanced by the net influx due to diffusion. This formalism is not realistic since it neglects the important role of resting voltage in striking the balance between influx and efflux of ions. Nevertheless, Appendix B demonstrates that, to a first approximation, c_i is spatially uniform, and we estimate deviations from spatial uniformity in the subsequent section The Approximate Pattern of Flow (see Fig. 4 *A*). The average value of c_i is related to the average intracellular hydrostatic pressure such that the integral of fluid flow across all membranes is zero

$$p_i = -RT(c_o - c_i). \quad (16)$$

This relationship implies that, for a concentration difference of 1 mM, i.e., $c_o - c_i = 1 \times 10^{-6}$ mol/cm^2, then $p_i = -20$ mmHg. Since animal membranes are thought to only be able to withstand a few mmHg of hydrostatic pressure, the average value of c_i must be very near to isotonic. Moreover, if the cell is an uninflated sack, then $p_i = 0$ and $c_i = c_0$.

In summary, c_i and p_i are essentially spatially uniform and their average values balance to produce no net driving force for transmembrane fluid movement. However, there must be small gradients in osmolarity to bring the water in across apical membranes and out across lateral membranes. The working osmotic gradients are estimated in the section on The Approximate Pattern of Flow.

TABLE I
PARAMETER VALUES

Constants	$RTc_o = 6 \times 10^3$ mmHg	$c_o = 0.3 \times 10^{-3}$ mol/cm^3	$\nu_w = 0.01$ cm^2/s
Dimensional	$\ell = 10 \times 10^{-4}$ cm	$\alpha = 1.0$	$w = 0.02 \times 10^{-4}$ cm
Morphometric	$S_m/V_T = 40 \times 10^3$ cm^{-1}	$V_c/V_T = 0.04$	$\tau = 0.05$
Surface area	$\xi_b^2 = 2$	$\xi_a^2 = 40$	$\ell S_m/V_T = 40$
Membrane	$L_m = 10^{-8}$ cm/(s mmHg)	$\omega_m = 10^{-7}$ cm/s	$n_m = 1.5 \times 10^{-11}$ mol/cm^{2}s
Solute diffusion	$D_S = 10^{-5}$ cm^2/s	$D_e = 2 \times 10^{-8}$ cm^2/s	$D_i = 10^{-5}$ cm^2/s $\quad \lambda_s = 22 \times 10^{-4}$ cm
Water Flow	$\eta_w = 6.4 \times 10^{-6}$ mmHg s	$\rho_e = 10^{10}$ mmHg s/cm^2	$\rho_i = 6.4$ mmHg s/cm^2 $\quad \lambda_w = 5 \times 10^{-4}$ cm
Dimensionless	$\frac{2}{\alpha}N_m = 3.3 \times 10^{-3}$	$0 \le \Omega_t \le \infty$	$\delta_e = 0.03 \quad \epsilon = 0.04$

Parameter values for the apical and basal membranes are presumably similar to the above membrane parameters. We define $\rho_i = \eta_w/\ell^2$. The tortuosity factor, τ, accounts for the added path length due to wiggling of the clefts and for narrowing of the clefts in local regions. Mathias (1983) shows that for uniform clefts $\tau = 1/\xi_m^2$. The chosen value is an arbitrary estimate based on studies of other tissues. The relationship of τ to D_e and ρ_e is derived in Appendix A.

Concentration and Pressure in the Lateral Intercellular Spaces

When δ_e and $(2/\alpha)N_m$ are both small numbers, the distribution of pressure is determined by combining Eqs. 14 to obtain

$$p_e(x) = \frac{1}{2}RTc_o\frac{2}{\alpha}N_m\left[1 - x^2/\ell^2 - \frac{\Omega_t}{1+\Omega_t}(1 - x/\ell)\right], \quad (17)$$

where $(2/\alpha)N_m$ is the normalized rate of active transport into the lateral intercellular spaces and Ω_t is the normalized permeability of the tight junctions; see Eq. 15 for their definitions.

If we consider two limiting situations, one where the tight junctions are infinitely permeable, $\Omega_t \to \infty$, and the other where the tight junctions are impermeable, $\Omega_t \to 0$, then we can bound the family of curves describing $p_e(x)$ for all values of Ω_t

$$\underset{\Omega_t \to 0}{(1 - x/\ell)x/\ell} \le p_e(x) \Big/ \left(RTc_o\frac{2}{\alpha}N_m\right) \le \underset{\Omega_t \to \infty}{(1 - x^2/\ell^2)}. \quad (18)$$

The envelope of this family of pressure profiles is shown in Fig. 2, and one intermediate profile is graphed for $\Omega_t = 1$.

The effect of the tight junction on fluid transport is determined by the value of the normalized permeability, Ω_t, which can be considered to be the ratio of two resistances: the resistance of ℓ cm of intercellular cleft to solute flux divided by the resistance of the junction to solute flux. However, the resistance of the intercellular spaces to solute flux is not simply related to diffusion. Eq. 15 implies the resistance of the lateral spaces is $\ell\rho_e/(RTc_o)$, which is a measure of their resistance to convection of solute. From Table I, we estimate $\ell\rho_e/(RTc_o) = 250$ s/cm. The value of the junctional resistance, $1/(\xi_t^2\omega_t)$, is related to the electrical resistance of the junction, $1/(\xi_t^2 g_t)$, by (Hodgkin and Katz, 1949)

$$1/(\xi_t^2\omega_t) = F^2c_o/(RT\xi_t^2 g_t).$$

Epithelia that are classified as leaky typically have transepithelial resistances of 5 to 500 Ω cm^2 (Schultz, 1977). If we arbitrarily choose the low value as representative of the junctional resistance, $(1/[\xi_t^2 g_t] = 5\ \Omega\ \text{cm}^2)$ then $\Omega_t = 0.04$. Thus, a 5 Ω cm^2 junction and a fairly narrow cleft ($w = 20$ nm) determine a pressure profile that looks as if the junction is tight to water flow. Wider clefts, or junctions with a higher electrical resistance will give even smaller values of Ω_t. From this analysis we conclude that the upper curve in Fig. 2 is likely to be representative of pressure profiles in most epithelia.

The concentration within a cleft is given by

$$c_e(x) = [p_e(x) + RTc_o]/RT. \quad (19)$$

Concentration profiles are therefore scaled and shifted versions of the pressure profiles, so Fig. 2 is easily interpreted in terms of $c_e(x)$ rather than $p_e(x)$. The deviations in

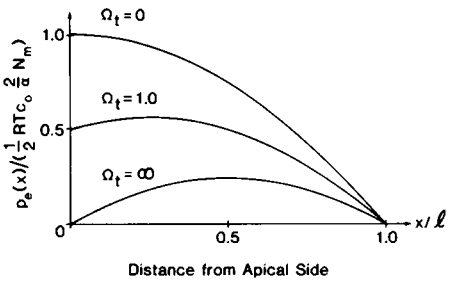

FIGURE 2 Profiles of hydrostatic pressure along the lateral intercellular space. The curves are described by Eq. 17. If we use the parameter values estimated in Table I, the value of the normalization is 0.5 RTc_o $(2/\alpha)N_m$ = 10 mmHg. The illustrated curves bound the pressure profiles for all values of the normalized junctional permeability, Ω_t. In the text we estimate $\Omega_t < 0.1$, in which case the upper curve accurately represents the pressure. The osmotic pressure within a cleft, $c_e(x) - c_o$, has the same profile and is calculated by substituting 10 mmHg $\to$ 0.5 mM.

concentration from isotonic can be expressed as a function of hydrostatic pressure,

$$c_e(x) - c_o = p_e(x)/RT$$

or

$$\Delta c_e = 5.3 \times 10^{-2}\ \text{mM/mmHg}.$$

For the values of hydrostatic pressure computed in Fig. 2, the concentration within the cleft is within 1 mM of isotonic everywhere.

The Approximate Pattern of Flow

The flow of water along all of the clefts in a unit area of tissue is given by

$$u_e(x) = -\frac{1}{\rho_e}\frac{dp_e(x)}{dx}.$$

Differentiating Eq. 17 and substituting dimensional parameters gives

$$u_e(x) = \ell\frac{S_m}{V_T}\frac{n_m}{c_o}\left[x/\ell - \frac{1}{2}\frac{\Omega_t}{1+\Omega_t}\right]. \quad (20)$$

It can be seen from Fig. 2 or Eq. 20 that the flow at the apical end of a cleft is directed out of the cleft and therefore reduces the net apical-to-basal water flux. As Ω_t varies from 0 to ∞, the outward flow at $x = 0$, $-u_e(0)$, varies from

$$\underset{\Omega_t \to 0}{0} \le -u_e(0) \le \underset{\Omega_t \to \infty}{\frac{1}{2}\ell\frac{S_m}{V_T}\frac{n_m}{c_o}}. \quad (21)$$

The total solute transport into the clefts is $\ell(S_m/V_T)\,n_m$, whereas the solute crossing the junctions is $c_o u_e(0)$. Thus, Eq. 21 shows that somewhere between 0 and 1/2 of the total solute flows back across the junctions, the value of 0 being approached when the junction is tight to fluid transport.

The longitudinal flow velocity, $u_e(x)$, and the transmembrane flow, u_m,

$$u_m(x) \equiv \frac{du_e(x)}{dx} \Big/ \frac{S_m}{V_T} \frac{cm^3}{cm^2\,s},$$

are illustrated in Fig. 3 *A* and *B*, for $\Omega_t = 1$. The pressure profile that corresponds to these flows is the intermediate curve illustrated in Fig. 2. Because hydrostatic pressure is essentially a quadratic function of x, the flow along the cleft is nearly linear in x, and the transmembrane flow is nearly a constant.

If we define the net driving force for transmembrane water flow (in units of osmotic pressure) by

$$\pi_{i,e} = c_{i,e} - c_o - p_{i,e}/(RT), \tag{22}$$

then to a first-order approximation

$$\pi_i = \pi_e \approx 0.$$

The transmembrane water flow is therefore driven by the small working standing osmotic gradients, $\delta\pi_{i,e}$, defined in the perturbation expansion by

$$\delta\pi_{i,e} = c_o\epsilon[C_{i,e}^{(1)} - P_{i,e}^{(1)}], \tag{23}$$

where ϵ is a small parameter and C, P are, respectively, the normalized concentration and pressure.

An analytical representation of $C_{i,e}^{(1)}$ and $P_{i,e}^{(1)}$ could not be found, but the equations, boundary conditions and integral constraints for these parameters allow us to sketch the net transmembrane driving force illustrated in Fig. 4 *A* and the resulting fluid flow sketched in Fig. 4 *B*. Fig. 4 is motivated by the following observations.

Since the lateral transmembrane water flow, u_m, is essentially independent of x, we have

$$\delta\pi_i(x, \alpha\ell) - \delta\pi_e(x) = n_m/(RTc_oL_m). \tag{24}$$

Both $\delta\pi_e(x)$ and $\delta\pi_i(x, r)$ are spatially varying parameters but their difference at the lateral membrane is constant. The x dependence of $\delta\pi_e(x)$ is due to x variations in extracellular hydrostatic and osmotic pressure. The x, r dependence of $\delta\pi_i(x, r)$ is due only to intracellular standing concentration gradients since the intracellular hydrostatic pressure is shown by Eq. B5 to be spatially uniform (probably zero) to three orders of approximation.

The fluid flow across apical membranes is

$$u_x(0, r) = \xi_a^2\, RTL_a\, \delta\pi_i(0, r). \tag{25}$$

The integral constraint on water flow is

$$(\alpha\ell)^2 \int_0^{\ell} \frac{S_m}{V_T} RTL_m[\delta\pi_i(x, \alpha\ell) - \delta\pi_e(x)]dx = 2\int_0^{\alpha\ell} \xi_a^2 RTL_a\delta\pi_i(0, r)rdr. \tag{26}$$

If we define the average working osmotic gradient across the apical membranes by

$$\delta\pi_a \equiv \frac{2}{(\alpha\ell)^2}\int_0^{\alpha\ell} \delta\pi_i(0, r)rdr, \tag{27}$$

then substituting the description of lateral membrane water flow (Eq. 24) into the integral constraint (Eq. 26) yields

$$\delta\pi_a = n_m/(c_oRTL_a). \tag{28}$$

Lastly, if we assume the junctions are tight to fluid flow, the boundary conditions on $\delta\pi_e(x)$ are

$$\delta\pi_e(0) = \delta\pi_e(\ell) = 0.$$

Since all of the transmembrane osmotic pressures scale with the lateral membrane solute transport rate, the sketches in Fig. 4 *A* are normalized by

$$n_m/(c_oRTL_m) = 0.25\ \text{mM}. \tag{29}$$

The average apical osmotic pressure then depends on the ratio L_m/L_a, but if we assume the membrane hydraulic conductivities are nearly equal, we have $\delta\pi_a \approx 0.25$ mM.

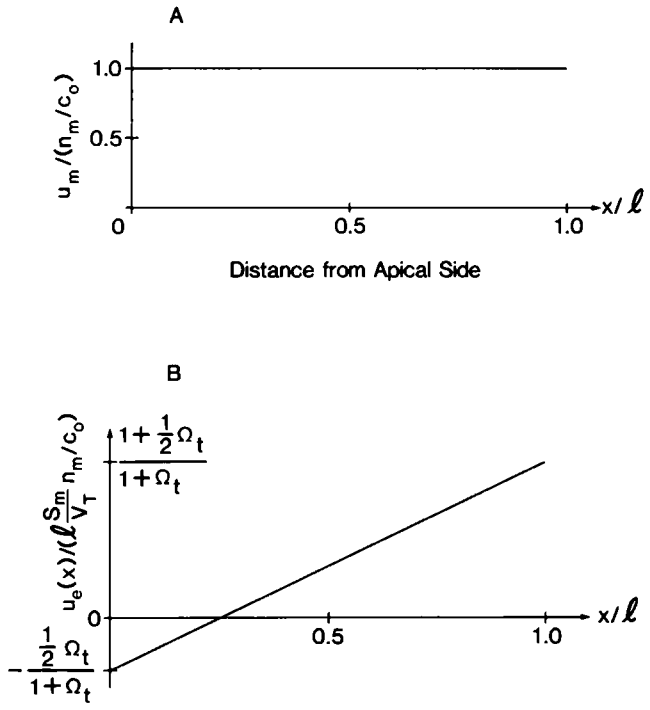

FIGURE 3 Profiles of the water flow into and along the lateral intercellular space. (*A*) The lateral transmembrane flow of water. For the parameter values in Table I, the normalization is $n_m/c_o = 5 \times 10^{-8}$ cm/s. (*B*) The total flow along all clefts in a unit cross-sectional area of epithelium. For the parameter values in Table I, the normalization is $(\ell S_m/V_T)n_m/c_o = 2 \times 10^{-6}$ cm/s. The cross-sectional area of the intercellular space is about 100 times smaller than a unit area of epithelium, hence the flow velocity along a single cleft is about 2×10^{-4} cm/s. To illustrate the dependence of the flow on Ω_t, we choose $\Omega_t = 1$ and indicate the dependence of the flow velocity, at $x = 0$ and $x = \ell$, on the value of Ω_t. This curve is described by Eq. 20.

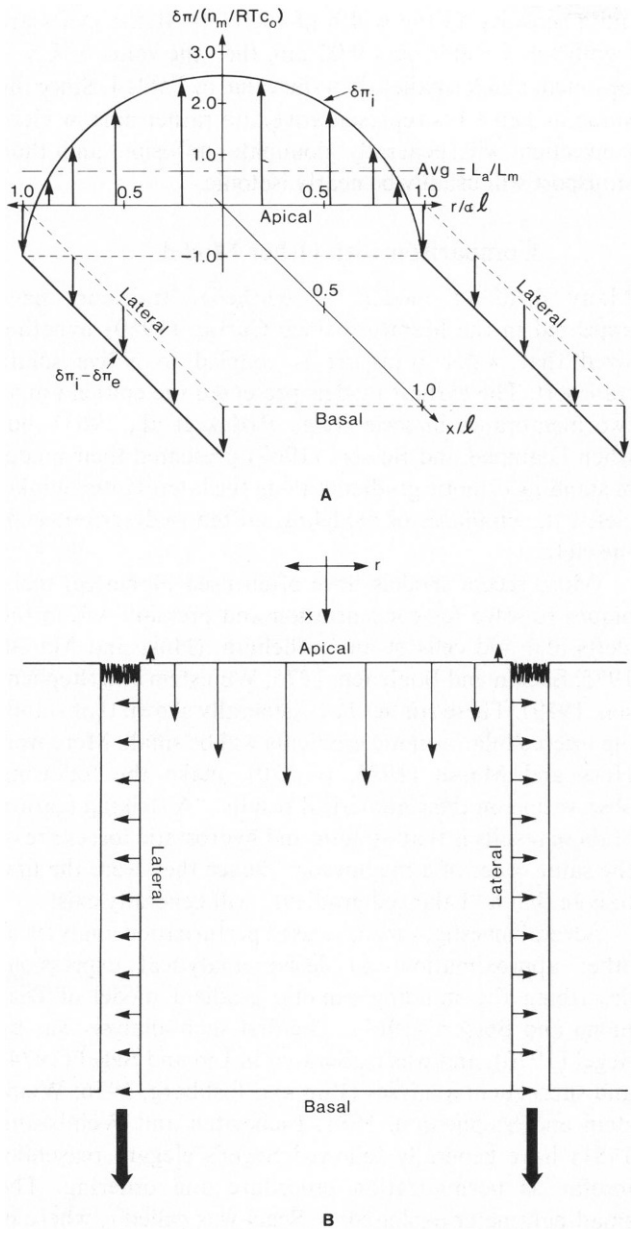

FIGURE 4 The net transmembrane osmotic pressure as a function of location in an epithelial cell. The arrows indicate the direction of water flow, upward for into the cells. Owing to the relatively small area of basal membrane, we assume basal flow is negligible and the average flows across apical and lateral membranes must balance. The apical transmembrane flow is generated by small standing concentration gradients within the cells, which bring the water into the cells. The water leaves the cells into the lateral intercellular spaces where hydrostatic pressure drives the longitudinal flow as illustrated in Figs. 2 and 3. However, the movement of water into the lateral spaces does not depend on the hydrostatic (or osmotic) pressure illustrated in Fig. 2, since this is the balanced gradient result and produces no net transmembrane driving force. The above graph illustrates the net working transmembrane osmotic pressure, which could not be analytically specified but must be close to the above sketch. (*B*) A sketch of the pattern of fluid movement (as shown by arrows) across the epithelial layer. This flow pattern is generated by the working osmotic gradients graphed in *A* and the arrows in either *A* or *B* are intended to represent the same fluid movement.

In summary, the lateral transmembrane water flow is essentially uniform and directed out of the cells whereas the apical membrane flow varies from outward at the cell periphery to inward at the cell center. Accordingly, the net osmotic pressure across lateral membranes is constant, whereas the apical pressure varies with radial location. In general, it is the distribution of standing osmotic gradients within the cells that sets the pattern of flow. In the cells, the flow velocity is relatively low, hydrostatic pressure gradients are very small, and standing concentration gradients build up to drive the transmembrane flow. The special role of the intercellular spaces is illustrated by Eq. 27, which shows that the net osmotic pressure across apical membranes is determined by the transport rate of solute across lateral membranes, implying that lateral transmembrane fluid flux is the rate limiting step in reabsorption.

DISCUSSION

Since the pioneering work of Diamond and Bossert (1967), investigators have looked for standing osmotic gradients in the lateral intercellular spaces but none have been found. Modern measurements of the membrane hydraulic permeability (Persson and Spring, 1982; Zeuthen, 1982) require that such gradients be rather small, so it is not surprising that they have not been measured. Nevertheless, the conventional view of transport (Spring, 1983) is that small standing osmotic gradients in the lateral spaces drive the reabsorption of fluid from the cells. The osmolarity within the cell is assumed to be uniform and hypertonic to the solution bathing the apical face of the epithelium, which drives the entry of fluid into the cells. The analysis presented here differs from this view on several points.

We find that the osmolarity within the cells is uniform but it is, on average, isotonic to the external bathing solution. Furthermore, to a first approximation the longitudinal standing osmotic gradients in the lateral spaces are balanced with standing gradients in hydrostatic pressure, so they too produce no net transmembrane driving force. The transmembrane driving forces are generated by small standing osmotic gradients within the cells (see Fig. 4 *A*). These results become intuitively reasonable if one considers that the fluid flow across lateral membranes must equal the apical flow. The intercellular compartment is small and tends to develop relatively large concentration and hydrostatic gradients, but the net transmembrane driving force at the lateral membranes cannot exceed that of the apical membranes.

To better understand the separation of the balanced gradient result from the working gradients it is useful to consider a quantitative example. In the Results section, we found that an electrically leaky epithelium, such as mammalian proximal tubule, is probably tight to fluid flow so that the upper curve in Fig. 2 is most likely correct. Accordingly, the extracellular hydrostatic pressure (see Table I) varies from 10 mmHg at the apical end of the

channel to 0 at the basal end, and this is balanced by an extracellular standing concentration gradient that varies from 0.53 mM to 0 over the same distance. Fluid reabsorption is driven by a uniform osmotic pressure across the lateral membranes of 0.25 mM, most of which is due to the intracellular compartment being slightly hypotonic at the lateral membrane surface (see Fig. 4 *A*). At the apical membrane we have an average intracellular osmotic pressure of 0.25 mM hypertonic, but, as illustrated in Fig. 4 *A*, the intracellular osmolarity varies from hypotonic at the periphery to hypertonic at the center. Thus, working standing osmotic gradients are mostly intracellular.

If we perform the thought experiment of somehow compressing the intercellular channel width by a factor of two yet keeping the rate of solute transport constant, then the rate of steady state fluid reabsorption will not change. However, the hydrostatic pressure in the intercellular channel will have to increase eightfold to drive the same volume of fluid through a channel of half the original volume and four times the original resistance. The increase in hydrostatic pressure will be balanced by an eightfold increase in osmotic pressure within the channel, hence the net steady-state lateral transmembrane driving force will remain 0.25 mM of osmotic pressure. The balanced gradient therefore ensures that fluid reabsorption is set by the rate of solute transport and not by the geometry of the channel.

Deviations from Isotonic Transport

In the analysis of extracellular fluxes presented in Eq. 1–4, the parameter δ_e scales the deviation of the transported fluid from isotonic. Substituting the balanced gradient result of Eq. 5 into the definition of osmolarity of the flow, Eq. 3, yields

$$\mathrm{os}(x) = \delta_e c_o + c_e(x). \tag{30}$$

At $x = \ell$, $c_e(\ell) = c_o$, hence the emergent osmolarity is

$$\mathrm{os}(\ell) = (1 + \delta_e)c_o. \tag{31}$$

Given the value of δ_e presented in Table I, the emergent osmolarity will be isotonic to within 3%, or to within 9 mM.

If the definitions of ρ_e and D_e (Eqs. A29 and A30) are substituted into Eq. 4 for δ_e, then we find

$$\delta_e = \frac{12 D_S \eta_w}{R T c_o w^2}. \tag{32}$$

The value of δ_e is determined by the effective resistance of the cleft to water flow divided by the effective resistance to solute diffusion (see Eq. 4). The dependence of δ_e on cleft width squared is analogous to the well-known result that the resistance of a pipe to water flow scales as the fourth power of the radius, whereas the amount of diffusive flux along a pipe depends only on the cross-sectional area, or on the second power of the radius. The value of δ_e is therefore quite sensitive to the width of the cleft. If the clefts are significantly wider than 0.02 μm, then the value of δ_e will be much, much smaller than the value in Table I. Since the value in Table I is representative of a rather narrow cleft, convection will generally dominate diffusion and fluid transport will usually be nearly isotonic.

Comparison with Other Models

Many different models of epithelial transport have appeared in the literature since Curran (1960) hypothesized that water transport is coupled to active solute transport. The earliest models presented the epithelium as two membranes in series (e.g., Patlak et al., 1963), but when Diamond and Bossert (1967) presented their model of standing osmotic gradients along the lateral intercellular clefts, the emphasis of modeling shifted to descriptions of the clefts.

More recent models have often used numerical techniques to solve for concentration and pressure within the clefts and and cells of an epithelium, (Huss and Marsh, 1975; Sackin and Boulpaep, 1975; Weinstein and Stephenson, 1979). These studies have generally shown that standing intercellular osmotic gradients will be small. Moreover, Huss and Marsh (1975, p. 320), make the following observation on their numerical results: "A striking feature of these results is that osmotic and hydrostatic forces are of the same order of a magnitude;" hence they were the first to note that a "balanced gradient" will generally exist.

Several investigators have used perturbation analyses or other approximations to derive analytical expressions describing the standing osmotic gradient model of Diamond and Bossert (1967). The first such analysis was by Segel (1970), and was elaborated in Lin and Segel (1974) and subsequent analyses (Lim and Fishbarg, 1976; Weinstein and Stephenson, 1981; Liebovitch and Weinbaum, 1981) have generally followed Segel's elegant reasoning insofar as normalization procedure and ordering. The small parameter exploited by Segel was called ν, where in present terminology

$$\nu = n_m/(c_o^2 R T L_m),$$

which gives a value from Table I of $\nu = 10^{-3}$. The ordering of parameters is therefore not a relevant difference between this analysis and that of Segel; rather, the important difference appears to be the inclusion of transmembrane hydrostatic pressure. Moreover, in Segel's analysis of Diamond and Bossert's equations, a parameter called κ is derived and for large values of κ he shows that the flow is dominated by convection. In terms of the nomenclature and parameters appearing in this analysis, κ is defined by

$$\kappa^2 = (\ell^2/\lambda_w^2)/\delta_e.$$

A large value of ℓ^2/λ_w^2 requires a balanced gradient and a small value of δ_e favors convection; the combination of

large ℓ^2/λ_w^2 and small δ_e ensures nearly isotonic transport. So even though Segel analyzed equations that neglect the important force of hydrostatic pressure, he was able to deduce the combination of parameters that governed flux along the cleft.

Most of the perturbation schemes have begun with the equations of Diamond and Bossert, so they automatically omitted hydrostatic pressure and considered only an isolated cleft. However, Liebovich and Weinbaum (1981) considered the entire epithelium and they point out the importance of requiring mass balance: yet they do not analyze intracellular gradients. Moreover, Liebovich and Weinbaum calculate the hydrostatic pressure within a cleft, but they do so by integrating the flow of water and do not consider how the water flow will be altered by transmembrane hydrostatic gradients. Thus, they did not include hydrostatic pressure as a driving force for the membrane water flow.

In general, all of the above models have focused on the intercellular channel as the site of distributed standing osmotic gradients and the intracellular space is treated as a lumped compartment. The analysis presented here shows that working osmotic gradients, those responsible for driving transmembrane flow, are largely due to distributed concentration gradients within the cells. Given a large value of membrane hydraulic conductivity, the working gradients are small, but fluid reabsorption is nonetheless dependent on them. A thorough numerical analysis of the intracellular osmolarity would be of some interest.

The weaknesses of the present analysis are: (*a*) voltage gradients and the effects of impermeant anions are neglected; and (*b*) analytical results have only been obtained for epithelia in symmetrical bathing solutions. McLaughlin and Mathias (1985) incorporate voltage into the analysis but focus on electro-osmosis and ignore other important effects. Work in progress on the lens incorporates voltage and impermeant anions, but the geometry of the lens is significantly different from that of other epithelia. Lastly, the effects of transepithelial gradients in voltage, concentration, or hydrostatic pressure need to be more adequately analyzed. Whenever such gradients exist, there will be accumulation/depletion of solute in the vicinity of the tight junctions and this situation induces local deviations from the balanced gradient. A preliminary analysis suggests that the technique of multiple scales (Cole, 1968) will yield an analytical solution to this problem, but a proper analysis, either analytical or numerical, awaits further work.

APPENDIX A

Equations for Solute and Water Flow in Extracellular Clefts

The purpose of this appendix is to take the equations that exactly describe conservation of matter, energy, and momentum in a continuum, and derive simpler equations for the flux of solute and water along the lateral intercellular spaces of an epithelium. The resulting equations are simpler inasmuch as some nonlinear terms are shown to be unimportant and the dimension of the extracellular flow problem is reduced from two to one. Moreover, the equations relate the physiologically important parameters of total flux per cm^2 of tissue, average transmembrane flux, and tissue morphometry.

In the cleft pictured in Fig. 5, the dimensions w, $\xi_m\ell$, and ℓ are assumed to be average dimensions of the tissue. The axial velocity of water flow at the membrane-water interfaces, $y = \pm w/2$, must be zero owing to viscous drag. Moreover, water and solute can cross membranes, so one has to a priori consider a normal (y directed) component of flow. A local y-z coordinate system is constructed (see Fig. 5), with z following the axis of the cleft and y normal to the axis.

Conservation of matter requires the divergence of flow equal zero. Namely,

$$\nabla \cdot v_e = 0, \tag{A1}$$

where $v_e = v_z(z,y)\,\mathbf{a}_z + v_y(z,y)\,\mathbf{a}_y$ is the vector describing the flow velocity within a cleft, furthermore we assume the flow profile is essentially the same in all celfts so variations occur only in the y-direction and z-direction of Fig. 5.

Conservation of energy and momentum in an incompressible viscous fluid is described by the Navier-Stokes equation (Landau and Lifshitz, 1959, p. 49).

$$\frac{1}{\nu_w}(v_e \cdot \nabla)v_e = -\frac{1}{\eta_w}\nabla p_e + \Delta v_e \tag{A2}$$

where p_e is the hydrostatic pressure in the extracellular clefts; η_w is the dynamic viscosity of water; ν_w is the kinematic viscosity of water; and the operator symbols ∇, $\cdot$, and Δ are defined specifically for the problem in hand by subsequent equations, or more generally in Landau and Lifshitz (1959).

The first step in simplifying these equations is to exploit the smallness of the ratio of cleft width to tissue width (see Fig. 5),

$$\epsilon^* = w/\ell \approx 10^{-4}.$$

Hence, the following normalizations are temporarily adopted:

$$\begin{aligned} Z &= z/\ell; \\ Y &= y/w. \end{aligned} \tag{A3}$$

which yield from Eq. A1

$$\epsilon^* \frac{\partial v_Z^*}{\partial Z} + \frac{\partial v_Y^*}{\partial Y} = 0 \tag{A4}$$

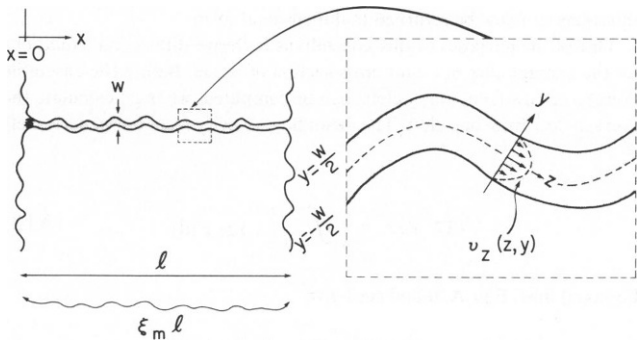

FIGURE 5 A definition of the coordinates and parameters used in the analysis of cleft flow. The *inset* shows the local coordinate system that is constructed within a cleft. The text shows that the flow of water along a cleft should be laminar, so the velocity profile illustrated in the *inset* is parabolic.

and from Eq. A2

$$(\epsilon^*)^2 R_e v_Z^* \frac{\partial v_Z^*}{\partial Z} + \epsilon^* R_e v_Y^* \frac{\partial v_Z^*}{\partial Y} + \frac{\partial P_e}{\partial Z} - (\epsilon^*)^2 \frac{\partial^2 v_Z^*}{\partial Z^2} - \frac{\partial^2 v_Z^*}{\partial Y^2} = 0, \quad \text{(A5)}$$

$$(\epsilon^*)^2 R_e v_Y^* \frac{\partial v_Y^*}{\partial Y} + (\epsilon^*)^3 R_e v_Z^* \frac{\partial v_Y^*}{\partial Z} + \frac{\partial P_e}{\partial Y} - (\epsilon^*)^3 \frac{\partial^2 v_Y^*}{\partial Z^2} - \epsilon^* \frac{\partial^2 v_Y^*}{\partial Y^2} = 0, \quad \text{(A6)}$$

where $(\epsilon^*)^2 R_e$, $\epsilon^* R_e$ are the Reynolds numbers, relative to this particular normalization, for Z, Y flow respectively; $u = RTc_o w^2/(\eta_w \ell)$ is the characteristic microscopic velocity of flow within a cleft, relative to this normalization of pressure; $v_e/u = v_Z^*(Z, Y)\,\mathbf{a}_Z + v_Y^*(Z, Y)\,\mathbf{a}_Y$; and $P_e = p_e/RTc_o$.

If it is now assumed that $\epsilon^* \simeq 0$, then from Eqs. A4–A6, respectively

$$\frac{\partial v_Y^*}{\partial Y} \simeq 0; \quad \text{(A7)}$$

$$\frac{\partial P_e}{\partial Z} \simeq \frac{\partial^2 v_Z^*}{\partial Y^2}; \quad \text{(A8)}$$

$$\frac{\partial P_e}{\partial Y} \simeq 0. \quad \text{(A9)}$$

Eq. A8 in conjunction with Eq. A9 defines the conditions of flow first analyzed by Poiseuille for laminar flow in a pipe or between parallel plates. Thus, the smallness of w/ℓ ensures Poiseuille flow even though we are dealing with semipermeable membranes lining wiggly clefts rather than impermeable parallel plates. Eq. A9 shows P_e is not a function of Y, so Eq. A8 can be integrated twice over Y to obtain

$$\frac{1}{2}\left(Y^2 - \frac{1}{4}\right)\frac{dP_e(Z)}{dZ} = v_Z^*(Z, Y), \quad \text{(A10)}$$

where the two constants of integration were determined by the boundary conditions on viscous flow, namely,

$$v_Z^*(Z, \pm 1/2) = 0. \quad \text{(A11)}$$

There is no further information in the normalized expansion, so the equations can now be returned to dimensional form.

One of the purposes of this appendix is to derive differential equations for the average flux in a unit cross section of tissue. Before the ensemble average of flow from many clefts can be computed, we must calculate the average flow from one cleft. The mean flow velocity from our generic cleft is

$$\langle v_z(z, y)\rangle = \frac{1}{w}\int_{-w/2}^{w/2} v_z(z, y)dy. \quad \text{(A12)}$$

For axial flow, Eqs. A10 and A12 give

$$\langle v_z(z, y)\rangle \triangleq \bar{v}_z(z) = -\frac{w^2}{12\eta_w}\frac{\partial P_e(z)}{\partial z}. \quad \text{(A13)}$$

This result represents the simplified Navier-Stokes equation for conservation of energy and momentum. One other simplified equation is required to ensure conservation of matter. If we perform the averaging procedure given by Eq. A12 on Eq. A1, the following result is obtained:

$$0 = \frac{1}{w}\int_{-w/2}^{w/2}\left[\frac{\partial v_z}{\partial z} + \frac{\partial v_y}{\partial y}\right]dy = \frac{\partial \bar{v}_z(z)}{\partial z} + \frac{1}{w}[v_y(z, w/2) - v_y(z, -w/2)], \quad \text{(A14)}$$

where the order of differentiation and integration was exchanged to compute the axial derivative of v_z. Moreover, the y components of velocity can be eliminated in favor of the membrane contribution to flow by

$$v_y(z, \pm w/2) = \pm u_m(z), \quad \text{(A15)}$$

where $u_m(z)$ is the transmembrane flow velocity in centimeters per second.

Substituting Eq. A15 into Eq. A14 yields an equation for axial water flow that is quite similar to the "cable" equation for ionic current flow along a nerve fiber (Hodgkin and Rushton, 1946) or along extracellular clefts of syncytia (Eisenberg et al., 1979)

$$\frac{\partial \bar{v}_z(z)}{\partial z} + \frac{2}{w}u_m(z) = 0. \quad \text{(A16)}$$

The above result is the simplified divergence equation that ensures conservation of water.

The last step is to refer the axial flow in a cleft to the average flow across 1 cm^2 of tissue and to put Eq. A16 into tissue coordinates. However, equations describing solute flux must also be derived and it is convenient to postpone the last step until both water and solute equations are available.

Conservation of solute requires that the divergence of the flux must be zero. By analogy with the steps used to obtain Eq. A16, we obtain

$$\frac{\partial \bar{j}_z(z)}{\partial z} + \frac{2}{w}j_m(z) = 0. \quad \text{(A17)}$$

The factors responsible for solute flux are diffusion and convection, thus

$$\mathbf{j}_e = D_S \nabla c_e(z, y) + c_e(z, y)\mathbf{v}_e(z, y) = j_z\mathbf{a}_z + j_y\mathbf{a}_y, \quad \text{(A18)}$$

where $c_e(z, y)$ is the concentration of solute in moles per centimeter cubed; D_S is the diffusion coefficient for solute in centimeters squared per second.

The average flux of solute $\bar{j}_z$ is computed by integrating the z component of Eq. A18 over y.

$$\bar{j}_z(z) = -D_S\frac{\partial \bar{c}_e(z)}{\partial z} + \frac{1}{w}\int_{-w/2}^{w/2} c_e(z, y)v_z(z, y)dy. \quad \text{(A19)}$$

The right-hand-most term of Eq. A19 is the average of the convected flux determined by averaging the product $\langle c_e v_z\rangle$, which is not in general equal to the product of the averages $\bar{c}_e\bar{v}_z$. $\langle c_e v_z\rangle = \bar{c}_e\bar{v}_z$ only if $c_e(z, y)$ is not a function of y, so that $c_e = \bar{c}_e$. The question is then: to what level of approximation, if any, can c_e be considered independent of y? The first step in answering this question is to exploit the smallness of w/ℓ.

Normalizing z and y in accordance with Eq. A3 and computing the divergence of Eq. A18 gives

$$0 = -\frac{D_S}{uw}\left[\frac{\partial^2 C_e}{\partial Y^2} + (\epsilon^*)^2\frac{\partial^2 C_e}{\partial Z^2}\right] + \frac{\partial}{\partial Y}(C_e v_Y^*) + \epsilon^*\frac{\partial}{\partial Z}(C_e v_Z^*), \quad \text{(A20)}$$

where

$$C_e(Z,Y) = c_e(z,y)/c_o.$$

Once again, assuming $\epsilon^* \simeq 0$, we find

$$\frac{\partial^2 C_e}{\partial Y^2} \simeq \frac{uw}{D_S}\frac{\partial}{\partial Y}(C_e v_Y^*). \tag{A21}$$

However, from Eq. A7 we see that v_Y^* is approximately independent of Y. The direction of v_Y^* at each membrane-water interface is inward, so either v_Y^* changes sign, in which case it cannot be independent of Y, or to the accuracy that we assume $\epsilon^* \simeq 0$ then so is $v_Y^* \simeq 0$. If this result is incorporated into Eq. A21, then it can be seen that

$$\frac{\partial^2 C_e}{\partial Y^2} = 0, \tag{A22}$$

which implies that C_e varies at most linearly with Y, but since C_e is also a symmetrical function of Y it must be independent of Y, which is the desired result

$$c_e(z,y) = \bar{c}_e(z). \tag{A23}$$

Since c_e is not a function of y, Eq. A19 can be integrated over y to obtain an average solute flux in terms of the average water flow.

$$\bar{j}_z(z) = -D_S\frac{\partial \bar{c}_e(z)}{\partial z} + \bar{c}_e(z)\bar{v}_z(z). \tag{A24}$$

The fluxes $\bar{j}_z$ and $\bar{v}_z$ are referred to a unit cross-sectional area of a generic cleft. To obtain the flow per unit area of tissue cross section, one must multiply the typical cleft flow by the fraction of cleft cross-sectional area in a unit cross section of tissue. The procedure for making this geometrical transformation is described in Mathias (1983). The result is

$$u_e(x) = -\frac{1}{\rho_e}\frac{dp_e(x)}{dx}; \tag{A25}$$

$$j_e(x) = -D_e\frac{dc_e(x)}{dx} - \frac{1}{\rho_e}c_e(x)\frac{dp_e(x)}{dx}; \tag{A26}$$

$$\frac{du_e(x)}{dx} + \frac{S_m}{V_T}u_m(x) = 0; \tag{A27}$$

$$\frac{dj_e(x)}{dx} + \frac{S_m}{V_T}j_m(x) = 0; \tag{A28}$$

where the effective resistance to water flow in the extracellular clefts is given by

$$\rho_e = \frac{12\eta_w/w^2}{\tau V_C/V_T}, \tag{A29}$$

and the effective diffusion coefficient for solute along the clefts is

$$D_e = D_S\,\tau V_C/V_T. \tag{A30}$$

The parameter V_C/V_T is the average volume of cleft in a unit volume of tissue; τ is the tortuosity factor, given by $\tau = 1/\xi_m^2$ for isotropic, unbranched clefts; and S_m/V_T is the average surface area of lateral membrane in a unit volume of tissue.

Although Eqs. A25–A30 have been derived for a simple epithelium, it can be shown that these results describe water and solute flow along intercellular clefts of other syncytial tissues, such as the lens or cardiac muscle, providing the size of the intercellular spaces are small relative to cellular dimensions. To apply these results to other tissues, one simply substitutes the tortuosity factor and morphometric parameters appropriate for the tissue of interest.

APPENDIX B

The Perturbation Analysis and Solution

The purpose of this appendix is to present the equations governing solute and fluid flow through epithelial tissue and to approximately solve these equations via a perturbation expansion. The perturbation in the parameter ϵ is based on two premises: (*a*) the size of the intercellular spaces is relatively small ($V_C/V_T = o[\epsilon]$); (*b*) the membrane permeability to water is relatively large ($\omega_m/[RTC_oL_m] \equiv \epsilon^2$). Furthermore, we have chosen an ordering of other terms in this expansion such that significant diffusional gradients can, at least in principle, build up in the lateral intercellular spaces. This analysis shows that significant standing intercellular osmotic gradients occur when convection of solute is rate limited by the large effective resistance to water flow exerted by very narrow clefts. We therefore assume the length constant for water flow is significantly shorter than the thickness of the epithelium, $\lambda_w^2/\ell^2 = o(\epsilon)$, (see Eq. 8), so we can assess the deviation in the fluid transport from isotonic.

GLOSSARY

Dimensionless Terms

$C = c/c_o$	normalized concentration;
$J = j/(c_o\mu_e)$	normalized solute flux;
$N = \xi^2 n/(c_o\mu_e)$	normalized rate of active transport;
$P = p/(RTc_o)$	normalized hydrostatic pressure;
$R = r/\ell$	normalized radial coordinate;
$U = u/\mu_e$	normalized water flow velocity;
$X = x/\ell$	normalized longitudinal coordinate;
$\Lambda = \xi^2 L/(\xi_m^2 L_m 2/\alpha)$	normalized hydraulic conductivity;
$\Omega = \xi^2\omega/\mu_e$	normalized solute permeability;
$\Pi = C - 1 - P$	normalized osmotic pressure;
$\sigma = 1 - \epsilon^2\Sigma$	reflection coefficient

where

$$\mu_e = \frac{RTc_o}{\rho_e\ell}\ (\text{cm/s}) \tag{B1}$$

is the characteristic flow velocity of water along all of the clefts in a unit area of epithelium relative to our normalization of pressure.

The above parameters will be subscripted according to their location within the epithelium. The subscripts have the same meaning as in the section on Equations of Flux, and they are defined there in the Glossary list Subscripts.

Some other dimensionless combinations of the dimensional parameters emerge in the process of normalizing the various equations, and these combinations have been assigned the following order in ϵ.

$$\begin{aligned} D_e\rho_e/(RTc_o) &= \delta_e \\ \lambda_w^2/\ell^2 &= \epsilon\lambda^2 \\ D_e/D_i &= \epsilon/D \\ \omega_m/(RTc_oL_m) &= \epsilon^2 \\ \mu_e\ell/\nu_w &= \epsilon^2/\nu \\ \rho_i/\rho_e &= \epsilon^3\rho. \end{aligned} \tag{B2}$$

Within the cells or along the lateral intercellular spaces, the flux of solute is due to diffusion and convection and the flow of water is related to hydrostatic pressure by the Navier Stokes equation (Landau and Lifshitz, 1959). Across membranes, solute may be actively transported, it may

diffuse down a concentration difference or it may be carried by water flow. Fluid can cross membranes due to an osmotic or hydrostatic pressure difference. The cells are assumed to be right circular cylinders, with wavy surfaces, of apparent length 1 and apparent radius α. Since at a given X location all clefts are assumed to have the same flow, there is no ϕ dependence in the problem. The resulting equations are

$$0 = \frac{d^2P_e(X)}{dX^2} + \frac{1}{\lambda^2\epsilon} \cdot \{P_i(X, \alpha) - P_e(X) + \sigma_m[C_e(X) - C_i(X, \alpha)]\}; \quad \text{(B3)}$$

$$0 = \delta_e \frac{d^2C_e(X)}{dX^2} + \frac{d}{dX}\left(C_e(X)\frac{dP_e(X)}{dX}\right) + \frac{\epsilon}{\lambda^2}[C_i(X, \alpha) - C_e(X)] + \frac{2}{\alpha}N_m + \frac{\epsilon}{\lambda^2}(1 - \sigma_m)C_m(X) \cdot \{P_i(X, \alpha) - P_e(X) + \sigma_m[C_e(X) - C_i(X, \alpha)]\}; \quad \text{(B4)}$$

$$\frac{\epsilon^5}{\nu}\left[\mathbf{U}_i(X, R) \cdot \nabla\right]\mathbf{U}_i(X, R) = -\frac{1}{\rho}\nabla P_i(X, R) + \epsilon^3\Delta\mathbf{U}_i(X, R); \quad \text{(B5)}$$

$$\mathbf{J}_i(X, R) = -\frac{\delta_e D}{\epsilon}\nabla C_i(X, R) + C_i(X, R)\mathbf{U}_i(X, R); \quad \text{(B6)}$$

$$0 = \nabla \cdot \mathbf{U}_i(X, R); \quad \text{(B7)}$$

$$0 = \nabla \cdot \mathbf{J}_i(X, R). \quad \text{(B8)}$$

Boundary conditions are based on the following assumptions. For the intercellular problem, we assume the clefts are open at the basal end but the apical end is occluded by a tight junction of arbitrary permeability. Within the cells, water flow tangential to a membrane is assumed to be zero owing to viscous drag, and water or solute flow normal to a membrane equals the transmembrane flow. For the lateral membranes, the transmembrane flow is related to the change in longitudinal flux by Eqs. B3 and B4, but these equations describe fluxes in a unit volume of tissue.[1] If we note that $S_m/V_T = \xi_m^2 2/(\alpha\ell)$, and then substitute for ξ_m^2 in the radial boundary conditions, we obtain Eqs. B18 and B19.

$$C_e(1) = 1; \quad \text{(B9)}$$

$$P_e(1) = 0; \quad \text{(B10)}$$

$$\frac{dP_e(0)}{dX} = \frac{\Lambda_t}{\epsilon}\{P_e(0) + \sigma_t[1 - C_e(0)]\}; \quad \text{(B11)}$$

$$\delta_e\frac{dC_e(0)}{dX} + C_e(0)\frac{dP_e(0)}{dX} = \Omega_t[C_e(0) - 1] + \frac{\epsilon}{\lambda^2}(1 - \sigma_t)\Lambda_t C_t\{P_e(0) + \sigma_t[1 - C_e(0)]\}; \quad \text{(B12)}$$

$$U_X(X, \alpha) = U_R(0, R) = U_R(\ell, R) = 0; \quad \text{(B13)}$$

$$-U_X(O, R) = \frac{\Lambda_a}{\epsilon\lambda^2}\{P_i(0, R) + \sigma_a[1 - C_i(0, R)]\}; \quad \text{(B14)}$$

$$-J_X(0, R) = \Omega_a[C_i(0, R) - 1] + N_a + \frac{1}{\epsilon\lambda^2}(1 - \sigma_a)C_a(R)\Lambda_a \cdot \{P_i(0, R) + \sigma_a[1 - C_i(0, R)]\}; \quad \text{(B15)}$$

$$U_X(1, R) = \frac{\Lambda_b}{\epsilon\lambda^2}\{P_i(1, R) + \sigma_b[1 - C_i(1, R)]\}; \quad \text{(B16)}$$

$$J_X(1, R) = \Omega_b[C_i(1, R) - 1] + N_b + \frac{\epsilon}{\lambda^2}(1 - \sigma_b)C_b(R)\Lambda_b \cdot \{P_i(1, R) + \sigma_b[1 - C_i(1, R)]\}; \quad \text{(B17)}$$

$$U_R(X, \alpha) = \frac{\alpha}{2}\frac{1}{\epsilon\lambda^2}\{P_i(X, \alpha) - P_e(X) + \sigma_m[C_e(X) - C_i(X, \alpha)]\}; \quad \text{(B18)}$$

$$J_R(X, \alpha) = \frac{\alpha}{2}\frac{\epsilon}{\lambda^2}[C_i(X, \alpha) - C_e(X)] + N_m + \frac{1}{\epsilon\lambda^2} \cdot (1 - \sigma_m)C_m(X) \cdot \{P_i(X, \alpha) - P_e(X) + \sigma_m[C_e(X) - C_i(X, \alpha)]\}. \quad \text{(B19)}$$

The differential equations and boundary conditions can be combined in integral form to put certain constraints on conservation of water and solute. Because these integral constraints are physically obvious conservation laws for the tissue, they are presented without rigorous justification. Nonetheless, they are rigorous consequences of the previous equations. The constraints which are subsequently used are

$$\frac{dP_e(0)}{dX} - \frac{dP_e(1)}{dX} = \frac{1}{\epsilon\lambda^2} \cdot \int_0^1 \{P_i(X, \alpha) - P_e(X) + \sigma_m[C_e(X) - C_i(X, \alpha)]\}dX; \quad \text{(B20)}$$

$$2\pi\alpha\int_0^1 U_R(X, \alpha)dX = -2\pi\int_0^\alpha [U_X(1, R) - U_X(0, R)]RdR; \quad \text{(B21)}$$

$$2\pi\alpha\int_0^1 J_R(X, \alpha)dX = -2\pi\int_0^\alpha [J_X(1, R) - J_X(0, R)]RdR. \quad \text{(B22)}$$

The last step is to seek a series solution to the equations of the form

$$C_{i,e}(X) = C_{i,e}^{(0)}(X) + \epsilon C_{i,e}^{(1)}(X) + \epsilon^2 C_{i,e}^{(2)}(X) + \ldots, \quad \text{(B23)}$$

$$P_{i,e}(X) = P_{i,e}^{(0)}(X) + \epsilon P_{i,e}^{(1)}(X) + \epsilon^2 P_{i,e}^{(2)}(X) + \ldots. \quad \text{(B24)}$$

The remainder of this Appendix will be spent solving these equations.

The Order Zero Distribution of Concentration and Pressure

The equations describing the various order problems are derived by first substituting the expansions given in Eqs. B23 and B24 into the flux equations and boundary conditions; then one simply collects all terms of

[1] The boundary conditions in Eqs. B11 and B12 are consistent with the balanced gradient condition of Eq. B35. However, if the reader wishes to apply more general boundary conditions (for example, the solute concentration in the bathing solution for the apical face could be other than unity), then the balanced gradient condition must break down near $x = 0$. The analytic specification of p_e and c_e then requires two expansions, one near $x = 0$, the other (balanced gradient) elsewhere. The solution of such a problem is derived by the technique of multiple scales (see Cole, 1968).

like power in ϵ. The order zero problem consists of those terms having no coefficient of ϵ

$$0 = P_i^{(0)}(X, \alpha) - P_e^{(0)}(X) + C_e^{(0)}(X) - C_i^{(0)}(X, \alpha) \quad \text{(B25)}$$

$$0 = \delta_e \frac{d^2C_e^{(0)}(X)}{dX^2} + \frac{d}{dX}\left(C_e^{(0)}(X)\frac{dP_e^{(0)}(X)}{dX}\right) + \frac{2}{\alpha}N_m \quad \text{(B26)}$$

$$0 = \nabla P_i^{(0)}(X, R) \quad \text{(B27)}$$

$$0 = \nabla C_i^{(0)}(X, R). \quad \text{(B28)}$$

Eqs. B27 and B28 imply that, to this order approximation, there is no spatial variation in intracellular pressure or concentrations, hence

$$P_i^{(0)} = \text{constant} \quad \text{(B29)}$$

$$C_i^{(0)} = \text{constant}. \quad \text{(B30)}$$

If we next invoke the integral constraint on fluid conservation (Eq. B21) for the order zero problem, then substituting Eq. B25 yields the relationship between intracellular concentration and pressure for no net fluid movement into or out of the cell

$$P_i^{(0)} = C_i^{(0)} - 1. \quad \text{(B31)}$$

Moreover, given that intracellular pressure and concentration are constants, we can differentiate Eq. B25 to obtain

$$\frac{dP_e^{(0)}(X)}{dX} = \frac{dC_e^{(0)}(X)}{dX}. \quad \text{(B32)}$$

Substituting Eq. B32 into Eq. B26 produces Eq. B33 which, although still nonlinear, can be integrated

$$0 = \frac{d}{dX}\left[\delta_e \frac{dC_e^{(0)}(X)}{dX} + C_e^{(0)}(X)\frac{dC_e^{(0)}(X)}{dX}\right] + \frac{2}{\alpha}N_m. \quad \text{(B33)}$$

Integrating Eq. B33 twice and applying the boundary conditions yields a quadratic equation in $C_e^{(0)}$. The positive root of this quadratic is presented in Eq. B39 where all of the order zero solutions are summarized.

We have thus far determined intracellular concentration and pressure to within an arbitrary constant. That constant can be evaluated by invoking the integral constraint given in Eq. B22. In summary, these results are

$$C_i^{(0)} = 1 - \frac{\frac{2}{\alpha}N_m + N_a + N_b}{\Omega_a + \Omega_b}; \quad \text{(B34)}$$

$$P_i^{(0)} = C_i^{(0)} - 1; \quad \text{(B35)}$$

$$C_e^{(0)}(X) = \left\{(\delta_e + 1)^2 + \frac{2}{\alpha}N_m(1 - X^2) - 2\Omega_t \cdot \left[\sqrt{(\delta_e + \Omega_t + 1)^2 + \frac{2}{\alpha}N_m} - (\delta_e + \Omega_t + 1)\right] \cdot (1 - X)\right\}^{1/2} - \delta_e; \quad \text{(B36)}$$

$$P_e^{(0)}(X) = C_e^{(0)}(X) - 1. \quad \text{(B37)}$$

If we define the net osmotic pressure that will drive fluid flow across membranes by

$$\Pi_{i,e} = C_{i,e} - 1 - P_{i,e}, \quad \text{(B38)}$$

we find

$$\Pi_i^{(0)} = \Pi_e^{(0)} = 0.$$

Thus, transmembrane fluid flow is driven by the small $\epsilon\Pi_{i,e}^{(1)}$ pressures. An analytical representation of the order one solutions could not be found, however, an approximate analysis is presented in the text in the Results section.

I would like to thank Drs. R. S. Eisenberg, S. McLaughlin, J. M. Diamond, and A. M. Weinstein for helpful discussions and a careful reading of this manuscript.

This work was supported in part by grants EY03095 and HL29205 from the National Institutes of Health and American Heart Association grant 79-851 with funds supported in part by the Chicago Heart Association.

Received for publication 20 July 1983 and in final form 8 January 1985.

REFERENCES

Berridge, M. J., and J. L. Oschman. 1972. Transporting Epithelia. Academic Press, Inc., New York.

Burg, M. B., and J. J. Grantham. 1971. Ion movements in renal tubules. *In* Membranes and Ion Transport. E. E. Bittar, editor. John Wiley & Sons, Inc., New York. 49–77.

Cole, J. D. 1968. Perturbation Methods in Applied Mathematics. Blaisdell, New York.

Curran, P. F. 1960. Na, Cl, and water transport by rat ileum in vitro. *J. Gen. Physiol.* 43:1137–1148.

Diamond, J. M., and W. H. Bossert. 1967. Standing-gradient osmotic flow. A mechanism for coupling of water and solute transport in epithelia. *J. Gen. Physiol.* 50:2061–2083.

Eisenberg, R. S., V. Barcilon, and R. T. Mathias. 1979. Electrical properties of spherical syncytia. *Biophys. J.* 25:151–180.

Hill, A. E. 1975. Solute-solvent coupling in epithelia: a critical examination of the standing-gradient osmotic flow theory. *Proc. R. Soc. Lond. B. Biol. Sci.* 190:99–114.

Hodgkin, A. L., and B. Katz. 1949. The effect of sodium ions on the electrical activity of the giant axon of the squid. *J. Physiol. (Lond.).* 108:37–77.

Hodgkin, A. L., and W. A. H. Rushton. 1946. The electrical constants of a crustacean nerve fibre. *Proc. R. Soc. Lond. B. Biol. Sci.* 133:444–479.

Huss, R. E., and D. J. Marsh. 1975. A model of NaCl and water flow through paracellular pathways of renal proximal tubules. *J. Membr. Biol.* 23:305–347.

Kaye, G. I., H. O. Wheeler, R. T. Whitlock, and N. Lane. 1966. Fluid transport in the rabbit gallbladder. *J. Cell Biol.* 30:237–268.

Kyte, J. 1976. Immunoferritin determinations of the distribution of $(Na^+ + K^+)$ ATPase over the plasma membranes of renal convoluted tubules. II. Proximal segment. *J. Cell Biol.* 68:304–318.

Landau, L. D., and E. M. Lifshitz. 1959. Fluid Mechanics. Pergammon Press, New York.

Liebovich, L. S., and S. Weinbaum. 1981. A model of epithelial water transport. *Biophys. J.* 35:315–338.

Lim, J. J., and J. Fischbarg. 1976. Standing-gradient flow — examination of its validity using an analytic method. *Biochem. Biophys. Acta.* 443:339–347.

Lin, C. C., and L. A. Segel. 1974. Illustration of techniques on a physiological flow problem. *In* Mathematics Applied to Deterministic Problems in the Natural Sciences. Macmillan Publishing Co., New York. 244–276.

Mathias, R. T. 1983. Effect of tortuous extracellular pathways on resistance measurements. *Biophys. J.* 42:55–59.

McLaughlin, S., and R. T. Mathias. 1985. Electro-osmosis and the reabsorption of fluid in renal proximal tubules. *J. Gen. Physiol.* In press.

Patlak, C. S., D. A. Goldstein, and J. F. Hoffman. 1963. The flow of solute and solvent across a two-membrane system. *J. Theor. Biol.* 5:425–442.

Persson, B., and K. R. Spring. 1982. Gallbladder epithelial cell hydraulic water permeability and volume regulation. *J. Gen. Physiol.* 79:481–505.

Sackin, H., and E. L. Boulpaep. 1975. Models for coupling of salt and water transport. Proximal tubular reabsorption in *Necturus* kidney. *J. Gen. Physiol.* 66:671–733.

Schultz, S. G. 1977. The role of paracellular pathways in isotonic fluid transport. *Yale J. Biol. Med.* 50:99–113.

Segel, L. A. 1970. Standing-gradient flows driven by active solute transport. *J. Theor. Biol.* 29:233–250.

Spring, K. R. 1983. Fluid transport by gallbladder epithelium. *J. Exp. Biol.* 106:181–195.

Sterling, E. S. 1972. Radioautographic localization of sodium pump sites in rabbit intestine. *J. Cell Biol.* 53:704–714.

Tisher, C. C., and J. P. Kokko. 1974. Relationship between peritubular oncotic pressure gradients and morphology in isolated proximal tubules. *Kidney Int.* 6:146–156.

Welling, L. W., and D. Welling. 1975. Surface area of brush border and lateral cell walls in the rabbit proximal nephron. *Kidney Int.* 8:343–348.

Welling, L. W., and D. Welling. 1976. Shape of epithelial cells and intercellular channels in the rabbit proximal nephron. *Kidney Int.* 9:384–394.

Weinstein, A. M. 1983. Nonequilibrium thermodynamic model of the rat proximal tubule epithelium. *Biophys. J.* 44:153–170.

Weinstein, A. M., and J. L. Stephenson. 1979. Electrolyte transport across a simple epithelium. *Biophys. J.* 27:165–186.

Weinstein, A. M., and J. L. Stephenson. 1981. Coupled water transport in standing gradient models of the lateral intercellular space. *Biophys. J.* 35:167–191.

Zeuthen, T. 1982. Relations between intracellular ion activities and extracellular osmolarity in *Necturas* gallbladder epithelium. *J. Membr. Biol.* 66:109–121.